Estimation of fractional coverage of alpine black soils by soybean vegetation using UAV-based multi-spectral images and vegetation indices

[1] Yun Jiang, [2, 3] Jun Wang* and [3] Jiwen Yang

[1] School of Public Administration and Law, Northeast Agricultural University, Harbin 150030, Heilongjiang, China
[2] College of Geo-Exploration Science and Technology, Jilin University, Changchun 130026, Jilin, China
[3] The Second Geomatics Cartography Institute, Ministry of Natural Resource, Harbin 150080, Heilongjiang, China

Received: 08.03.2023

Abstract. To extract accurately and quickly the fractional vegetation coverage (FVC) for the case of soybean crops in alpine black-soil regions during flowering-podding and seed-filling growth stages, we use unmanned aerial vehicles (UAVs) to collect multi-spectral images of the soybean crops. Different vegetation indices for the multi-spectral bands are analyzed and compared. These are a vegetative index (VEG), a colour index of vegetation extraction (CIVE), an excessive green-feature index (EXG), an excessive green-and-red difference index (EXGR), a combined vegetation index (CVI), a normalized green-blue difference index (NGBDI), a normalized vegetation index (NDVI), a soil-adjusted vegetation index (SAVI), and a modified soil-adjusted vegetation index (MSAVI). A supervised classification method is combined with a threshold method based on statistical histograms of the vegetation indices. This offers an efficient technique for extracting the soybean coverage in the alpine black soils. We divide our experimental field into soil pixels and soybean pixels, while the UAV-based remote-sensing data is divided into the categories of soil and soybean vegetation, using a supervised classification method. Then intersects of the histograms of the vegetation-indices distributions derived with the UAV data are taken as thresholds for the soil and soybean-vegetation pixels. The soybean FVC extracted from synchronously collected high-resolution visible-light images with the ground resolution 0.036 m is used as a reference value for the comparative analysis of the accuracies. Our study reveals the following: (1) the FVC-extraction accuracy becomes higher than 90% if the thresholds of the vegetation indices are determined by the statistical histograms and the images obtained with the UAVs are classified in order to extract the FVC, (2) one obtains too high a coverage with the NGBDI index; the corresponding errors are equal to 6.14% and 2.18% respectively for the flowering-podding and seed-filling stages, (3) the COM, VEG, EXG, SAVI and MSAVI indices demonstrate a sufficient accuracy and reliability, and (4) the EXG index provides the highest precision at the podding stage, while the COM index is the best for the period of soybean-kernel filling. Our results represent an important reference for future high-precision extraction of the soybean-vegetation coverage at different growth stages.

Keywords: multi-spectral images, soybean crop, vegetation indices, unmanned aerial vehicles (UAVs)

UDC: 004.932.2

1. Introduction

Fractional vegetation coverage (FVC) reflects a degree to which an above-ground vegetation covers a soil area. Usually, it is determined as the ratio of the vertical projection area of above-ground vegetation organs (including stems, leaves and branches) to the total vegetation area on a soil (usually expressed in per cents) [1, 2]. In such applied fields as construction and testing of ecological models, e.g. hydrology and climate ones, the FVC is an important factor for monitoring,

*Corresponding author

analyzing and describing the state of vegetation growth [3, 4]. Moreover, it has a great significance for crop monitoring and disaster assessment [5–7].

Up to date, the common methods for measuring the FVC [8, 9] include mainly remote-sensing estimations and near-ground measurements [10, 11]. Due to the limitations of temporal and spatial resolutions [12, 13], satellite-based remote-sensing estimation of images is mainly suitable for large-scale monitoring of vegetation. It hardly meets the needs of crop-coverage monitoring at the scales of separate fields. Near-ground measurement methods [14, 15] are generally used within small areas. They are characterized by high operating costs and can easily damage the crops [16–18]. In recent years, aerial-photography technologies based upon unmanned aerial vehicles (UAVs) are increasingly maturing. Their main features are high flexibility, simple operation, low flight requirements and easy control of temporal and spatial resolutions. This explains wide utilization of the above technologies in the studies of small-scale regional agricultural production, vegetation-information extraction and some other applications [19–21].

Many scholars have already examined the UAV-based remote-sensing technology for the extraction of vegetation coverage. Choi et al. [22] have estimated the vegetation coverage in some dune areas, using a random-forest classification and a normalized vegetation index (NDVI) obtained from multi-spectral UAV images. Liu Yanhui et al. [23] have analyzed the FVC for large grasslands, using an excessive green-feature index (EXG) and a colour index, and reported that the accuracy for the UAV images is high enough if the EXG index is estimated by the maximum-entropy method based on a genetic algorithm. Zhao Jing et al. [4] have extracted the FVC of maize during four different growth periods in summer, using visible-light UAV images and employing a visible difference-vegetation index, an EXG and a normalized green-blue difference index (NGBDI). It has been found that the results derived with the EXG index are the best. Due to Xie Bing et al. [24], a red-green-blue vegetation index (RGBVI) has been suggested for the high-precision UAV-based extraction of FVC for small areas. The reliability and the accuracy of the method have also been verified.

Although a lot of studies have been carried out on the FVC extraction from the multi-spectral and visible-light UAV-obtained images, most of them select only two or three different vegetation indices and address only single-stage grasslands or crop regions. Moreover, only a few studies have been reported on the FVC extraction for the soybeans at different stages of their growth. The problem is that the vegetation indices differ at different growth stages due to different spectral reflectances of soybeans and soil background.

In the present study, we take Nenjiang City, an area of alpine black soils in Heilongjiang Province, as an experimental area. Both visible-light and multi-spectral UAV images of the soybean crops have been collected during two different periods of growth. By analyzing and comparing our experimental data, we have estimated the FVC for our experimental area, using a common vegetation index suitable for the visible spectral range. The sample photographic data for the field is then combined to analyze the extraction results obtained with different vegetation indices. Our final aim is to find the most reliable methods of FVC extraction for the soybean crops at different growth periods.

2.2. Materials and methods

2.1. Area under study and data sources

Nenjiang City is an important area for soybean production in Heilongjiang Province. The area studied in our experiments is located in the east of Nenjiang City (125°40′40″–125°40′47″E and

49°6′31″–49°6′35″N). It is characterized by a cold-temperate continental monsoon climate, with the average annual temperature 0.8–1.4°C, the average annual precipitation between 480 and 512 mm, and the accumulated temperature greater than or equal to 10°C being about 2340°C. Soybeans have been planted by machines.

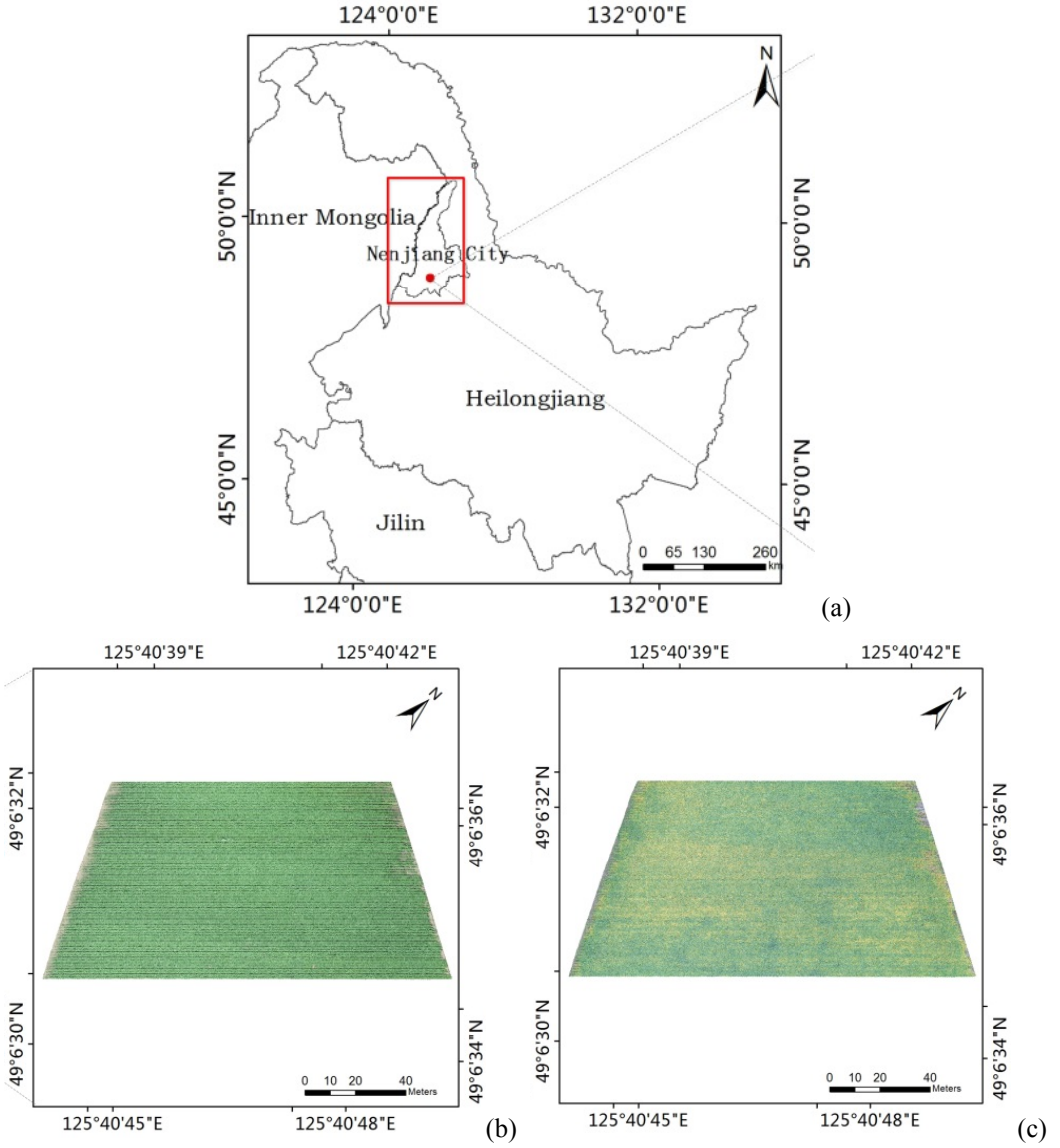

Fig. 1. Area under study: location of the area (a) and images of the sample area taken on July 23rd (b) and September 3rd (c).

2.2. Data acquisition and processing

The images were collected on July 23 and September 3, 2020. They correspond to the flowering-podding and seed-filling stages of soybeans, respectively (see Fig. 1). Due to COVID-19, the data for the flowering-podding stage was collected a little bit later, and the collection time referred to the middle and late soybean flower-pod period. The UAV-obtained visible-light images, which had been used for verification, were acquired using a DJI Phantom 4 RTK UAV. The main parameters of the UAV are gathered in Table 1. The UAV-obtained multi-

spectral data used in the test were acquired by DJI M600 equipped with an Altum UAV multi-spectral sensor (produced by MicaSense). The multi-spectral sensor that integrated infrared and visible images with high resolution was able to detect five visible and infrared bands between 475 nm and 840 nm. The spatial resolution reached 5.2 cm at the altitude 120 m. The corresponding main parameters are also shown in Table 1.

The UAV-based visible images of the soybean fields had been collected between 11:00 and 13:00 on sunny days with no clouds and breeze at the following flight parameters: the flight height 70 m, the flight speed 4 m/s, the side overlaps 80%, the heading overlap 80%, and the ground resolution 0.036 m. The flight route was automatically planned (the 1st time) and fixed (the 2nd time). The flight height used for obtaining the multi-spectral images with the UAV was equal to 100 m and the ground resolution was 0.05 m. The general overview of the field is shown in Fig. 1. In this study, Pix4D software was employed to process the visible images collected by the UAVs. After importing aerial photos with POS information into the software, the pre-collected coordinates of the image-control points were imported by manual puncturing. Then we generated the UAV-obtained visible image of the experimental area through point-cloud encryption, feature-point matching, texture-feature matching, etc. In case of he multi-spectral images, we calculated the spectral reflectances using a combination of image data, a standard whiteboard and ENVI. Based on the POS data obtained by the UAVs, the Pix4D software was used for stitching processing of the multi-spectral images.

Table 1. Main parameters of our UAV.

Parameter	Multi-spectral channels	Thermal infrared channel
Resolution	2064×1544	160×120
Lens focal length	8 mm	1.77 mm
Field of view	48°×36.8°	57°×44.3°
Spatial resolution (at the flying altitude 120 m)	5.2 cm	81 cm
Channel wavelength	Blue: 465–485 nm Green: 550–570 nm Red: 663–673 nm Red-edge: 712–722 nm NIR: 820–860 nm	8–14 μm
Volume and weight	82×67×64.5 mm^3 (357 g)	82×67×64.5 mm^3 (357 g)

Digital photos of the field were collected manually and visible images were obtained by the UAVs. Thirty-four sampling points were arranged in the experimental area at the intervals 15–20 m and the sampling range for each sampling point was equal to 90×90 cm^2 (with wiring by staff before photographing). At the centre of each sampling point, a tablet (Huawei Brand) had been used to take photos vertically downward in order to minimize geometric deformation errors at the height 60 cm from the top of the crop. 1 to 3 photos had been taken at each sampling point to ensure that there were no people or other objects in the photos.

2.3. Method for extraction FVC for the soybean crops

The reflection characteristics of soybean canopy and soil in the blue, green, red, red-edge and near-infrared bands obtained from the experimental area during the flowering-podding and seed-filling stages are shown in Fig. 2. From comparison of the data, we conclude that the soybean canopy has a small reflection peak in the green band of the Altum UAV multiple-spectral sensor and a strong reflection in the near-infrared region, with the reflectivity about 0.7. There is a reflectance valley inside the red band, while the reflection inside the red and blue bands is weak. The soil characteristics are relatively gentle and the corresponding reflection increases when passing from blue to green, red, red-edge and near-infrared bands. This reflectance is smaller than that of the soybean canopy in all the bands except for the red band where it is slightly higher. The reflectance difference is about 0.6 in the near-infrared band, which is consistent with the studies performed on the wheat canopy and the appropriate soils [3].

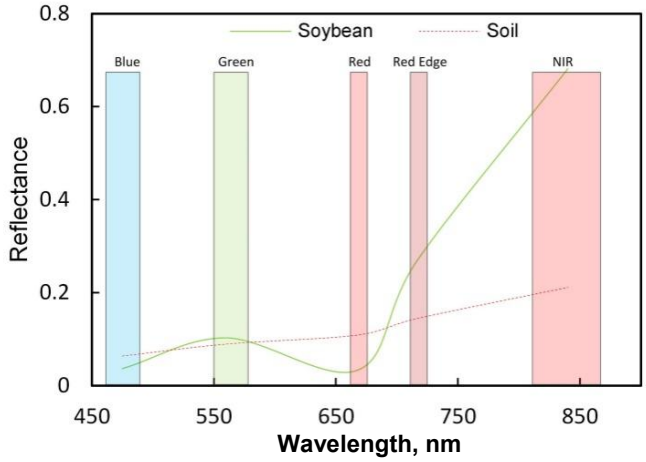

Fig. 2. Typical spectral curves of soybeans and soil that correspond to (a) flowering-podding and (b) seed-filling stages.

In application to green-vegetation monitoring, the vegetation indices can better reflect the spectral characteristics of green vegetation based upon multi-band spectral calculations. More than 40 kinds of the vegetation indices have been used in the branches of vegetation studies and ecology (see also Section 1). They include NDVI, an enhanced vegetation index (EVI), and a new

vegetation index (NVI). From the viewpoint of the spectral characteristics of soybeans and soils, a vegetative index (VEG) [25], a colour index of vegetation extraction (CIVE) [26], an EXG [27], excessive-green and excessive-red difference indices (EXGR) [28], a combined vegetation index (CVI) [29] and an NGBDI [30, 31] have been selected. The aim is better detection of strong reflection of green light by green vegetation. An NDVI, a soil-adjusted vegetation index (SAVI) and a modified soil-adjusted vegetation index (MSAVI) [32] have been selected to detect better the characteristics of the red and near-infrared bands. In total, 12 vegetation indices can be used to extract the soybean-vegetation coverage. Specific formulae for the vegetation indices used by us are shown in Table 2. In the above formulae, ρ_B , ρ_G , ρ_R and ρ_{NIR} are the reflectances respectively in the blue, green, red and near-infrared bands ($\rho_R = \frac{R}{R+G+B}$, $\rho_G = \frac{G}{R+G+B}$, $\rho_B = \frac{B}{R+G+B}$ and $\rho_{NIR} = \frac{NIR}{R+G+B+NIR}$).

The methods commonly used for estimating the vegetation coverage, which are based on the remote-sensing data, are mainly divided into three categories: empirical methods, hybrid pixel models and machine-learning methods [11]. The empirical method needs establishing a statistical relationship between the FVC and the vegetation index based on a large number of reliable sample data. It is difficult to do in the case of FVC estimation at large scales [33]. The threshold approach to the vegetation index, which is widely used in the mixed pixel model, considers that each pixel can be divided into vegetation and non-vegetation [14]. The intersection method for the vegetation-index time-series graphs have been applied to determine a classification threshold for the UAV-obtained images of winter wheat and summer corns. It can achieve good enough results [3, 4]. In the present study, we use the UAV multi-spectral remote-sensing technology and the vegetation-index threshold method. It is based on selecting the nine vegetation indices described above to estimate the soybean FVC in the alpine black-soil region. The relevant extraction process is illustrated in Fig. 3.

Table 2. Formulae used for calculating different vegetation indices.

Vegetation index	Formula	Reference
VEG	$VEG = \frac{\rho_G}{\rho_B^{(1-\alpha)} \times \rho_R^{\alpha}}$, $\alpha = 0.667$	[25]
CIVE	$CIVE = 0.441\rho_R - 0.811\rho_G + 0.385\rho_B + 18.78745$	[26]
EXG	$\mathrm{EXG} = 2\rho_\mathrm{G} - \rho_\mathrm{R} - \rho_\mathrm{B}$	[27]
EXGR	$XRG = 3\rho_G - 2.4\rho_R - \rho_B$	[28]
CVI	$CVI = 0.25EXG + 0.3EXGR + 0.33CIVE + 0.12VEG$	[29]
NGBDI	$NGBDI = \frac{\rho_G - \rho_B}{\rho_G + \rho_B}$	[31]
NDVI	$NDVI = \frac{\rho_{NIR} - \rho_R}{\rho_{NIR} + \rho_R}$	[33]
SAVI	$SAVI = \frac{\rho_{NIR} - \rho_G}{\rho_{NIR} + \rho_G + L}(1+L)$ (L is soil conditioning factor, o.5)	[33]
MSAVI	$MSAVI = \frac{2\rho_{NIR} + 1 - \sqrt{(2\rho_{NIR}+1)^2 - 8(\rho_{NIR} - \rho_R)}}{2}$	[33]

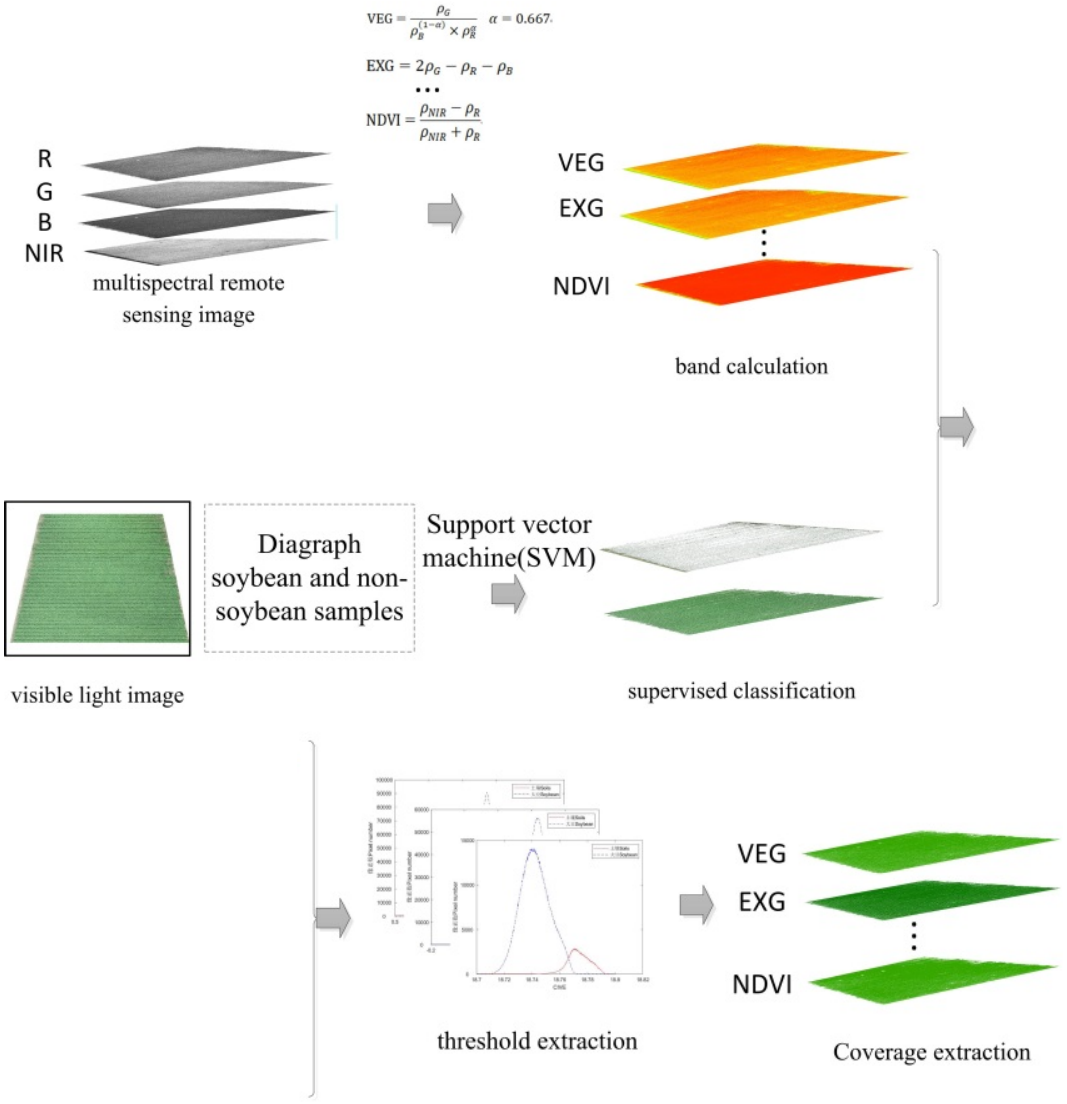

Fig. 3. Flow chart of FVC extraction for soybean crops.

The experimental field in the area under study is divided into two parts: soil pixels and soybean pixels. Then the UAV multi-spectral data is divided into soil and soybean vegetation, using a supervised classification performed with the support vector machine (SVM). The intersection of the distribution histograms for a given vegetation index is derived with the UAV multi-spectral data as a threshold for the soil and soybean-vegetation pixels. Then the image parts with the values larger than the classification threshold correspond to the soybean-vegetation pixels. Otherwise, they correspond to the soil pixels. Finally, the FVC is extracted based on the classification results.

The relation used for extracting the FVC by the vegetation-index threshold method is given by

$$F_{\text{soybean}} = \frac{N_{\text{soybean}}}{N_{\text{soybean}} + N_{\text{soil}}} \times 100\%, \tag{1}$$

where N_{soybean} is the number of the soybean pixels and N_{soil} the number of the soil pixels.

2.4. Accuracy evaluation for the soybean-crop FVC

A commonly known method for evaluating the FVC accuracy takes the coverage measured by the ground photography as a true FVC value. However, it is unsuitable for FVC evaluating on large scales due to the limitations of material resources. As the remote UAV-based sensing and deep-learning technologies develop, a combination of high-resolution UAV images and supervised SVM classification can provide the information on the FVC with high precision so that the results of supervised classification can be used as a true coverage value.

Here we use the high-resolution visible-light remote-sensing images, while the parameters measured for the field samples are verified through the supervised SVM classification. Then the data obtained due to classification is used as a true value of the soybean FVC. As a result, the accuracy of the soybean FVC extracted from the image can be evaluated. The parameters measured for the field samples are extracted manually from the photos obtained for the field using Photoshop software. First, the colour range is used to extract the soybean range and then a further manual refinement is performed with 'magic wand' and 'lasso' tools. Three persons extract independently their photographs of soybean samples and the final result for each sample point is the average of these three results. To avoid human errors caused by supervised classification as much as possible, three people perform the supervised SVM classification of the remote-sensing visible-light data and the final classification results are averaged. The accuracy-evaluating parameters used for the soybean-related FVC extraction read as

$$mean\ \ absolute\ \ error = \frac{\sum_{i=0}^{n}\left|x_i - x_i^{'}\right|}{n}, \tag{2}$$

$$variance = \frac{1}{n-1}\sum_{i=1}^{n}\left(x_i - x_i^{'}\right)^2, \tag{3}$$

$$accuracy = 1 - \frac{\left|x_i - x_i^{'}\right|}{x_i} \times 100\%, \tag{4}$$

where x_i denote the estimated values of the FVC at the sample points, $x_i^{'}$ the reference values of the FVC at the sample points, and n is the number of the sample points.

3. Results and discussion

3.1. Classification and processing of high-resolution visible-light remote-sensing data

Our data source is the high-resolution visible-light remote-sensing data with the ground resolution 0.036 m. It is collected synchronously from the multi-spectral images acquired on July 23, 2020. The SVM-supervised classification is then used. Thirty samples of soil and thirty samples of soybeans have been selected from the experimental area to be divided into a soybean coverage area and a non-soybean coverage area after preprocessing, field investigation and image interpretation. To verify the accuracy of supervised classification, we calculate the confusion matrix for the two classification results. The overall classification accuracy is equal to 98.73% and the Cohen's kappa coefficient is 0.972 (see Table 3).

To verify the FVC accuracy for the visible-light images, the digital photos collected for the field have been manually extracted by Photoshop. Then the average has been taken as a reference value. The measured values and the data of supervised classification for different sampling points are shown in Fig. 4. Here the mean absolute error amounts to 0.0189, the variance is 0.00046 and the accuracy equals to 97.99%.

Table 3. Evaluation of supervised classification for soybean coverage.

Item	Soybean, pixels	Soil, pixels	Total	User accuracy, %
Soybean, pixel	4337	72	4409	98.37
Soil, pixel	12	2210	2222	99.46
Total	4349	2282	6631	
User accuracy, %	99.72	96.84		
	The total accuracy is 98.73% and the Cohen's kappa coefficient is 0.972			

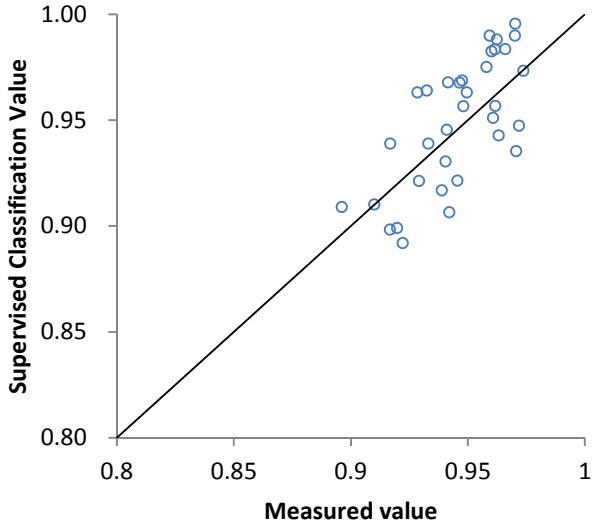

Fig. 4. Comparison of the results obtained from measurements and supervised classification.

3.2. Threshold extraction and analysis

The method for extracting the FVC based on the vegetation indices uses a threshold for binary processing so that the extraction of this threshold is an important part of the experiments. In this study, we have selected 30 soil samples and 30 soybean samples from the experimental area to be divided into soybean-covered and non-soybean-covered areas using the method of supervised classification. Based on the classification results, the vegetation indices of the corresponding areas have been calculated. Then the statistical analysis has been carried out according to a method of histograms, where the intersection of the statistical histograms is used as a classification threshold.

Using the classification results and the statistical analysis, we have calculated the vegetation indices VEG, CIVE, EXG, EXGR, CVI, NGBDI, NDVI, SAVI and MSAVI for the soybean crops during the flowering-podding and seed-filling stages. The appropriate histograms are shown in Fig. 5 and Fig. 6. The intersect of the soil and vegetation curves in the extracted statistical histograms has been used as the extraction threshold for the corresponding vegetation index (see Table 4).

Basing on the statistical histograms, one can conclude that the spectral reflectances of the vegetation and the soil have evident double-peak characteristics. The spectral reflectance changes notably depending on the growth period. The thresholds also depend on the growth period. In particular, the threshold for the CIVE index shifts towards greater values and that for the other indices shifts towards smaller values during the period of seed filling (see Table 4).

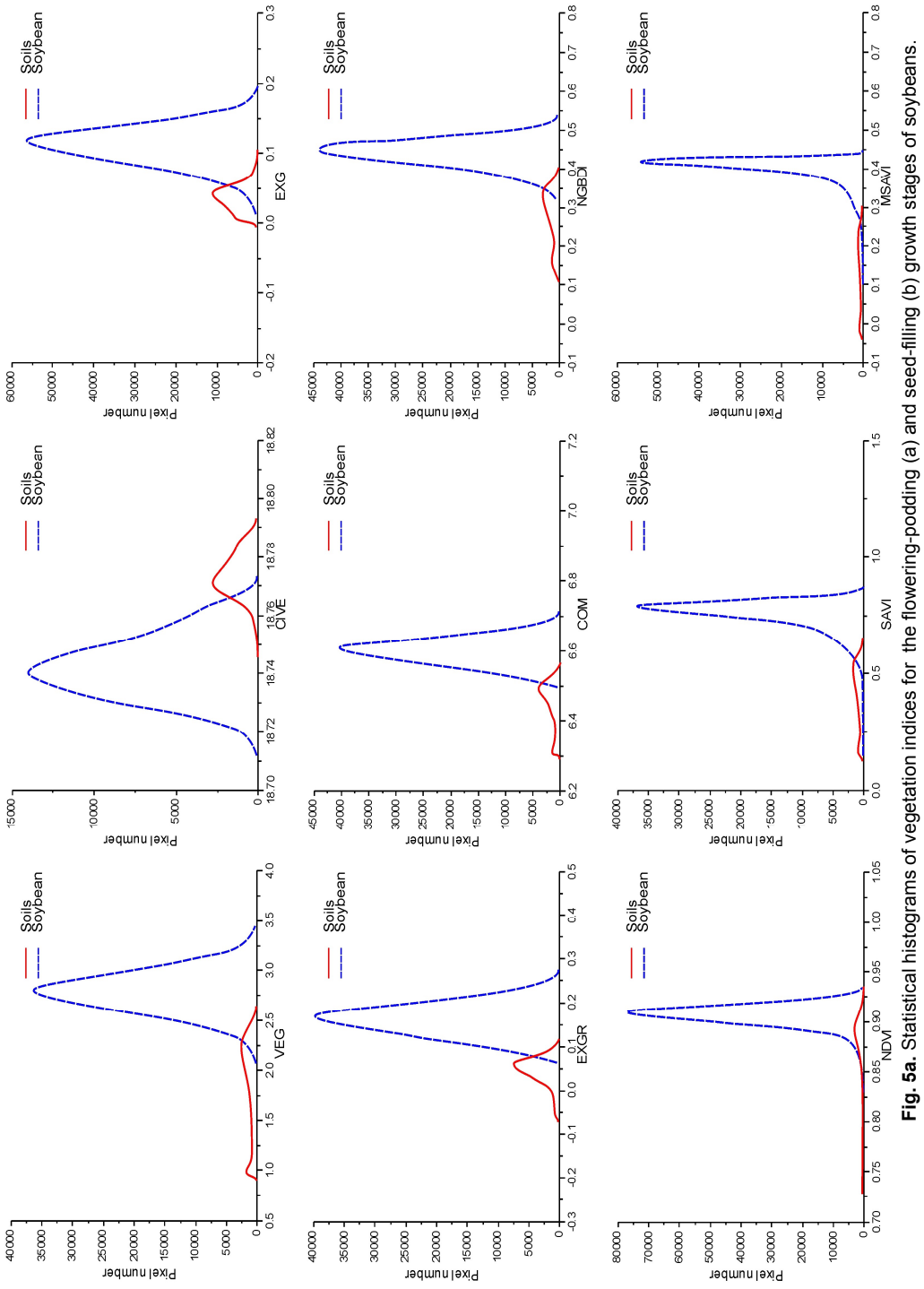

Fig. 5a. Statistical histograms of vegetation indices for the flowering-podding (a) and seed-filling (b) growth stages of soybeans.

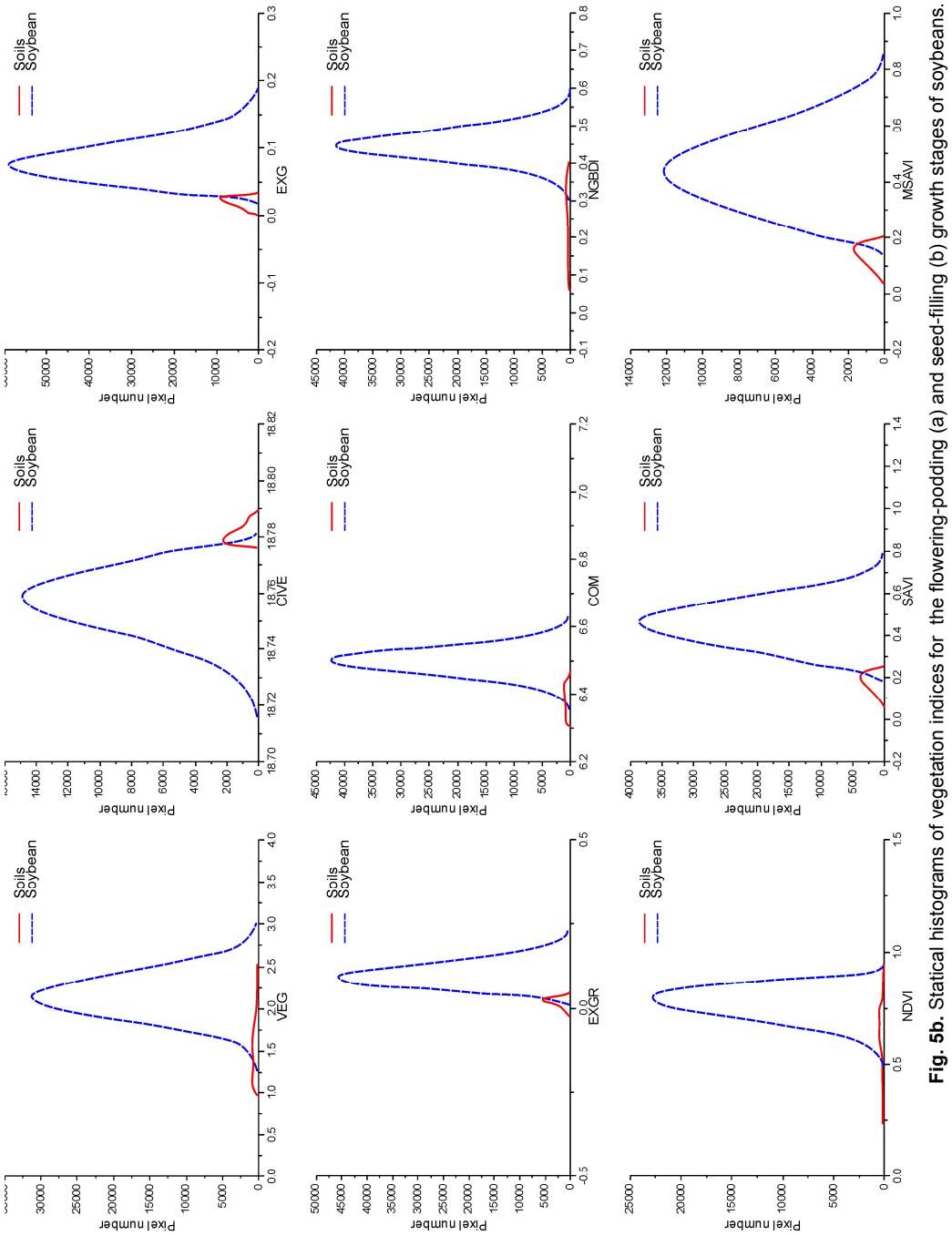

Fig. 5b. Statical histograms of vegetation indices for the flowering-podding (a) and seed-filling (b) growth stages of soybeans.

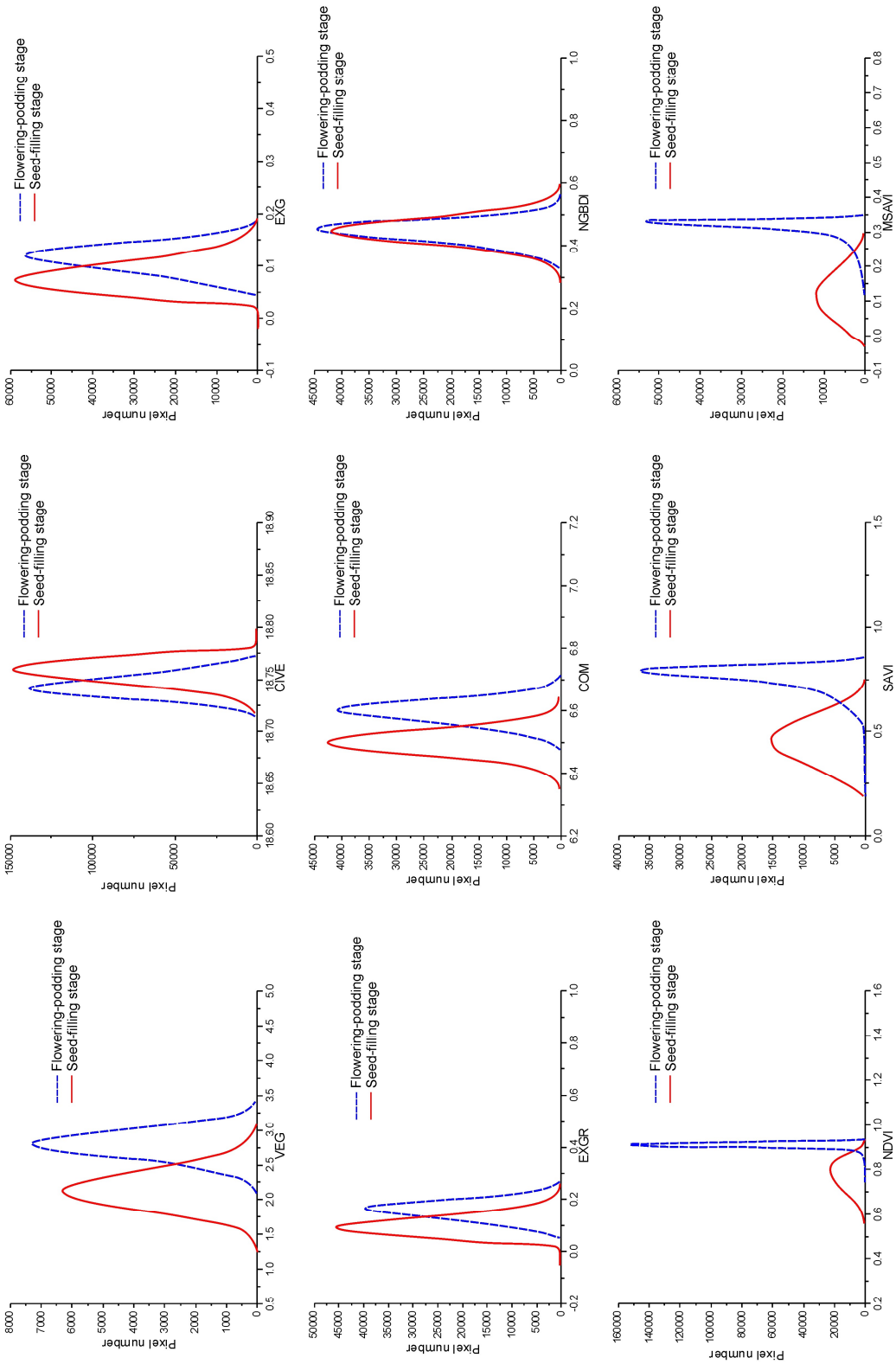

Fig. 6. Statistics of the changes observed for soybean-vegetation indices.

Table 4. Extraction thresholds obtained for different vegetation indices.

Vegetation index	Threshold value for the vegetation index	
	Flowering-podding stage	Seed-filling stage
VEG	2.285	1.375
CIVE	18.766	18.777
EXG	0.054	0.027
EXGR	0.074	0.028
CVI	6.505	6.381
NGBDI	0.349	0.318
NDVI	0.869	0.515
SAVI	0.561	0.220
MSAVI	0.585	0.179

3.3. Extracted results and analysis of soybean FVC

The vegetation index for the multi-spectral UAV images has been calculated for the two periods based on the formulae mentioned above and the classification resulted from the thresholds. Fig. 7 and Fig. 8 show the vegetation coverages extracted by various vegetation indices for the flowering-podding and seed-filling stages. Green is the vegetation coverage area, and white is the non-vegetation coverage area. It can be seen from the classification results that there are some gaps between the ridges in the images of vegetation during the flowering-podding stage (July 23), although they are almost completely covered during the period of seed filling (September 3). The FVC is then obviously higher than that during the flowering-podding stage. The flowering-podding stage is a rapid growth stage of soybean plants. On the other hand, the growth is slow during the period of seed filling, especially during the period of vigorous reproductive growth with partial yellow-green leaves. The changes observed in the FVC basically conform to the rules of growth of soybean plants during these periods.

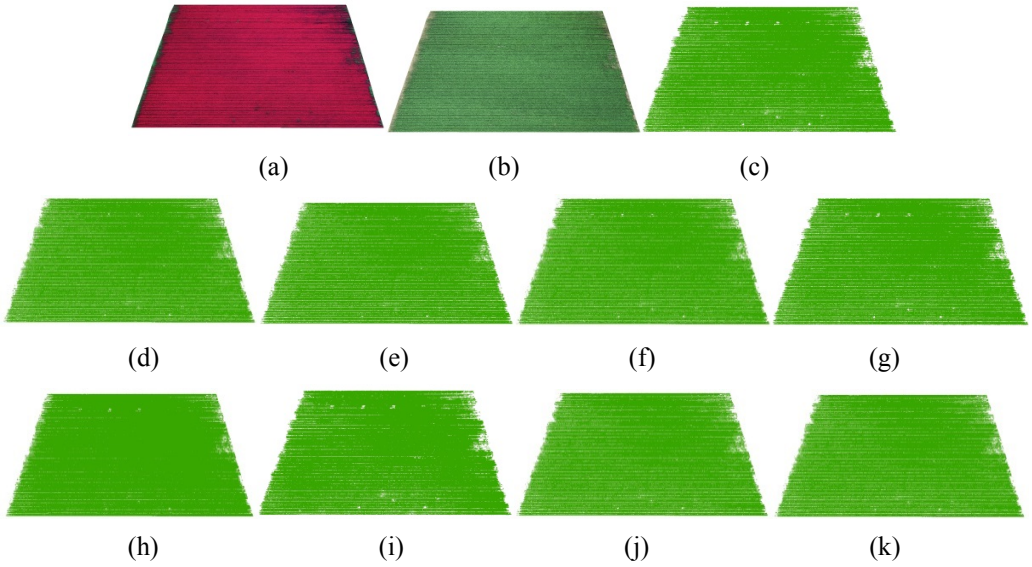

Fig. 7. Classification images (panels a, b) and results (panels c–k) obtained for the flowering-podding period: (a) a multi-spectral image, (b) a corresponding visible-light image, (c) VEG, (d) CIVE, (e) EXG, (f) EXGR, (g) CVI, (h) NGBDI, (i) NDVI, (j) SAVI, and (k) MSAVI.

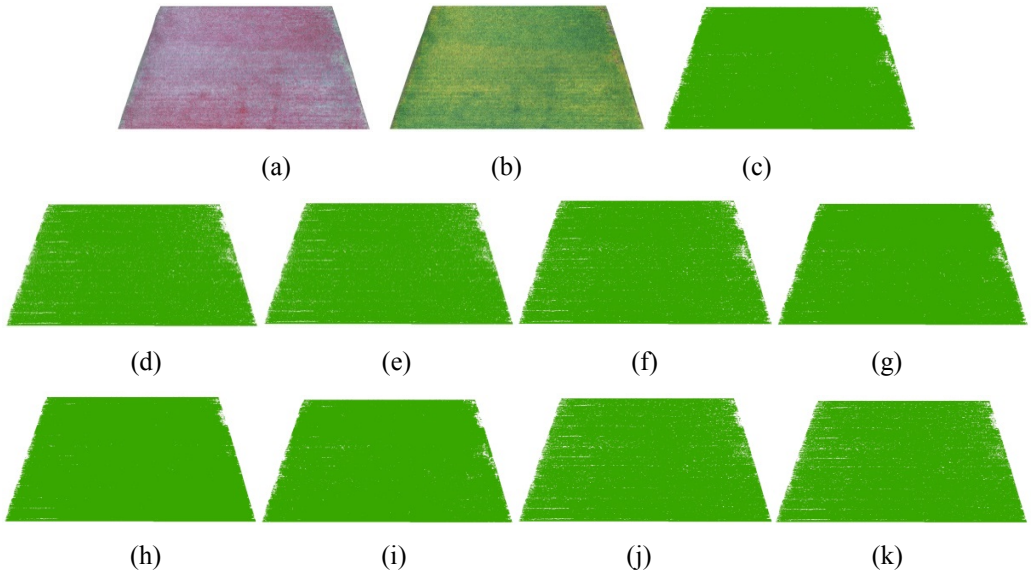

Fig. 8. Classification images (panels a, b) and results (panels c–k) obtained for the seed-filling period: (a) a multi-spectral image, (b) a corresponding visible-light image, (c) VEG, (d) CIVE, (e) EXG, (f) EXGR, (g) CVI, (h) NGBDI, (i) NDVI, (j) SAVI, and (k) MSAVI.

To evaluate the accuracy for the soybean FVC obtained by the index-threshold method, we determine the average of the supervised SVM-classification data obtained by three individuals as a true soybean FVC. Then the formula for the FVC error is as follows:

$$\mathrm{E}_F = \frac{\left|F_{\sup} - F_{V1}\right|}{F_{\sup}} \times 100\%, \tag{5}$$

where E_F implies the FVC-extraction error, $F_{\sup}$ the soybean FVC extracted with the supervised-classification method, and F_{V1} the soybean FVC extracted with the vegetation-threshold method.

The FVC values have been calculated using different vegetation-index methods. As seen from Table 5, the FVC ranges from 87% to 94% during the flowering-podding stage and reveals notable data fluctuations. The difference of the maximal and minimal values is 6.81%. If we compare our results with the data obtained by the supervised classification, one can see that the accuracy is over 94%. Moreover, the absolute EXG error is the lowest and the absolute NGBDI error is the highest. The FVC mostly lies in the region 95–99% during the seed-filling stage. The soybean FVCs extracted by different vegetation indices are very close to each other, with small enough fluctuations (e.g., the difference between the highest and lowest values is only 2.28%). A comparison with the FVC extracted by the supervised classification shows that the absolute CVI error is the lowest and the absolute NGBDI error is the highest. As follows from the results derived for the two growth periods, the CVI and VEG accuracies are high enough. They are followed by the EXG, SAVI and MSAVI accuracies. A comparison with the statistical NGBDI-histogram data testifies that the applicability of NGBDI for the FVC extraction based on the threshold of the statistical histogram is not sufficiently high. Fig. 9 displays the extraction accuracy described as a scatter FVC plot (see Eq. (5)). It has been obtained by the supervised-classification and vegetation-index threshold methods.

As follows from Fig. 9, it is better to extract the soybean FVC using the UAV multi-spectral images and the vegetation-index threshold method. This refers to both the flowering-podding and

Table 5. Calculation results obtained for soybean FVC.

Vegetation index	Soybean growth stage	Vegetation index threshold method, %	Supervised classification, %	Error extraction, %	Absolute error, %
VEG	Flowering-podding stage	89.32	88.64	0.77	0.68
	Seed-filling stage	98.20	97.42	0.80	0.78
CIVE	Flowering-podding stage	91.00	88.64	2.66	2.36
	Seed-filling stage	95.97	97.42	1.49	–1.45
EXG	Flowering-podding stage	88.42	88.64	0.25	–0.22
	Seed-filling stage	95.92	97.42	1.54	–1.50
EXGR	Flowering-podding stage	87.27	88.64	1.55	–1.37
	Seed-filling stage	95.97	97.42	1.49	–1.45
CVI	Flowering-podding stage	87.92	88.64	0.81	–0.72
	Seed-filling stage	97.80	97.42	0.39	0.38
NGBDI	Flowering-podding stage	94.08	88.64	6.14	5.44
	Seed-filling stage	99.54	97.42	2.18	2.12
NDVI	Flowering-podding stage	90.83	88.64	2.47	2.19
	Seed-filling stage	98.93	97.42	1.55	1.51
SAVI	Flowering-podding stage	87.10	88.64	1.74	–1.54
	Seed-filling stage	96.79	97.42	0.65	–0.63
MSAVI	Flowering-podding stage	91.03	88.64	2.70	2.39
	Seed-filling stage	96.73	97.42	0.71	–0.69

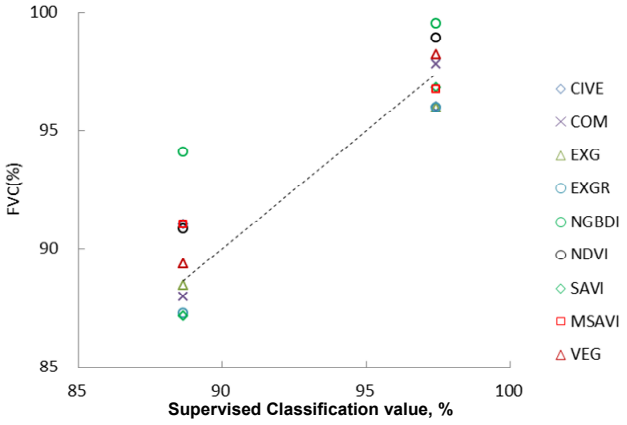

Fig. 9. Scatter plot obtained for the FVC-extraction results.

seed filling stages. The results obtained with the CVI, VEG and EXG classification thresholds are the closest to the supervised-classification data, while the NGBDI-classification threshold results are the most distant from the supervised-classification data. The FVC remains lower during the flowering-podding stage. Then the nine FVC-classification thresholds differ greatly from those of

the seed-filling stage. During the period of seed filling, the FVC is higher and the nine FVC-classification thresholds are smaller. When the plants grow, the reflectance of the soybean leaves increases and each of the vegetation indices gets saturated to a certain extent. This is basically consistent with the earlier results reported in the literature for wheat and corns. Deep reasons of this correspondence still need to be explored. If compared with the supervised-classification results, the soybean FVCs estimated by the classification thresholds for the nine vegetation indices are larger. This can be associated with smaller classification thresholds obtained as intersects of the vegetation-indices statistical histograms. Therefore these results are more consistent with the data obtained for the winter-wheat FVC [3].

3.4. Further verification of FVC accuracy

To further verify the FVC accuracy based on the vegetation-indices approach, we extract manually the digital photos collected on the field using Photoshop, with the mean value as a reference. The indicators shown in Table 6 reveal that the accuracies of the nine vegetation indices used in our study are all above 90%.

Table 6. Accuracy parameters of the FVC estimation for sample points.

Method	Flowering-podding stage			Seed-filling stage		
	Mean absolute error	Variance	Accuracy, %	Mean absolute error	Variance	Accuracy, %
VEG	0.041	0.00179	95.62	0.014	0.00063	98.48
CIVE	0.024	0.00046	97.43	0.048	0.00353	95.01
EXG	0.027	0.00058	97.14	0.050	0.00375	94.83
EXGR	0.026	0.00054	97.22	0.038	0.00233	96.08
CVI	0.038	0.0014	95.94	0.016	0.00070	98.25
NGBDI	0.044	0.00137	95.28	0.052	0.00406	94.62
NDVI	0.044	0.00140	95.32	0.054	0.00429	94.46
SAVI	0.019	0.00026	98.03	0.011	0.00057	98.76
MSAVI	0.018	0.00023	98.12	0.017	0.00083	98.13

The FVC accuracy for the flowering-podding stage is the highest in case of the MSAVI index, with the smallest variance and the highest stability. It is followed by the SAVI, CIVE, EXGR, EXG, CVI and VEG indices. Finally, the accuracy of the NGBDI index remains the lowest. For the seed-filling stage, the FVC accuracy is the highest for the VEG index. It provides the smallest data fluctuations. Then the CVI, MSAVI, SAVI and EXGR indices follow. The lowest accuracy is typical for the NDVI index. In general, the CVI, VEG, EXG, SAVI and MSAVI indices manifest a sufficiently high accuracy and good stability. The soybean FVCs estimated by the classification thresholds for the nine vegetation indices at the sampling points are generally higher than the coverages measured by the ground-photography method. This fact is consistent with the previous results obtained using the supervised-classification data.

4. Conclusions

Summing up the main results of this study, one can draw the following conclusions.

(1) The statistical histograms have been used to determine the thresholds vegetation–soil for

different vegetation indices. On this basis, the UAV multi-spectral images have been classified to extract the FVC values. The appropriate accuracy can be as high as 90%. Therefore it is feasible to use common vegetation indices to extract the vegetation coverage.

(2) A comparison of the classification results demonstrates that the FVC extracted from the NGBDI index is more reliable than the values obtained with the other vegetation indices. Comparing the data associated with the NGBDI index and the statistical histograms, one can see that the NGBDI index is not suitable for implementation of this method.

(3) A comparison of the soybean FVCs obtained from the UAV images, the vegetation indices and the corresponding measured reference value testifies that the accuracy of FVC extraction associated with the CVI, VEG, EXG, SAVI and MSAVI indices is sufficiently high. The appropriate parameters reveal a satisfactory stability and are the closest to the true FVC value. This refers to both soybean-growth periods.

(4) Comparing the soybean FVC extraction during the two different growth periods, one concludes that different vegetation indices perform differently for these periods. The extraction accuracy of the EXG index is the highest for the flowering-podding stage and the extraction accuracy of the CVI index is the highest for the period of seed filling. As a consequence, the automatic extraction of soybean FVC demands appropriate selection of the vegetation index according to the growth characteristics of the vegetation during different periods.

(5) Comparing the coverage values measured by the ground-photography method and the results of supervised classification, one testifies that the results for the soybean FVC estimated using the nine vegetation-index classification thresholds are generally higher. This is caused by a smaller classification threshold obtained as the intersect of the vegetation-index statistical histograms. Since the resolution (0.036 m) of the UAV images in this study is not high enough, some of the soil pixels or those of 'mixed' areas pixels (e.g., edge pixels and small gaps between leaves) are classified as the vegetation pixels.

Data availability. The experimental data used to support the findings of this study are available from the corresponding author upon request.

Conflicts of interest. The authors declare that they have no conflicts of interest regarding this work.

Funding statement. The present study was funded by the State Key Laboratory of Geo-Information Engineering and the Key Laboratory of Surveying and Mapping Science and Geospatial Information Technology of MNR, CASM (2021-03-10).

References

1. Yue J, Guo W, Yang G, Zhou Ch, Feng H and Qiao H, 2021. Method for accurate multi-growth-stage estimation of fractional vegetation cover using unmanned aerial vehicle remote sensing. Plant Meth. **17**: 51–55.
2. Purevdorj T, Tateishi R, Ishiyama T and Honda Y, 1998. Relationships between percent vegetation cover and vegetation indices. Int. J. Remote Sens. **19**: 3519–3535.
3. Niu Y X, Zhang L Y, Han W T and Shao G M, 2018. Fractional vegetation cover extraction method of winter wheat based on UAV remote sensing and vegetation index. Trans. Chin. Soc. Agricult. Mach. **49**: 212–221.
4. Zhao J, Yang H B, Lan Y B, Lu L Q, Jia P and Li Z M, 2019. Extraction method of summer corn vegetation coverage based on visible light image of unmanned aerial vehicle. Trans. Chin. Soc. Agricult. Mach. **50**: 232–240.
5. Qi J, Marsett R C , Moran M S , Goodrich D C, Heilman P, Kerr Y H, Dedieu G, Chehbouni A and Zhang X X, 2000. Spatial and temporal dynamics of vegetation in the San Pedro River basin area. Agricult. Forest. Meteorol. **105**: 55–68.

6. Owen T W, Carlson T N and Gillies R R, 1998. An assessment of satellite remotely-sensed land cover parameters in quantitatively describing the climatic effect of urbanization. Int. J. Remote Sens. **19**: 1663–1681.
7. Hu H, Li N, Tian F and Tie Q, 2018. Modification of harmonic analysis model for diurnal surface soil heat flux estimate from multiple remote sensing data. J. Appl. Remote Sens. **12**: 036009.
8. Xu N, Tian J, Tian Q, Xu K and Tang S, 2019. Analysis of vegetation red edge with different illuminated/shaded canopy proportions and to construct normalized difference canopy shadow index. Remote Sens. **11**: 1192.
9. Goodwin A W, Lindsey L E, Harrison S K and Paul P A, 2018. Estimating wheat yield with normalized difference vegetation index and fractional green canopy cover. Crop, Forage & Turfgrass Management. **4**: 1–6.
10. Song W, Mu X, Ruan G, Gao Z, Li L and Yan G, 2017. Estimating fractional vegetation cover and the vegetation index of bare soil and highly dense vegetation with a physically based method. Int. J. Appl. Earth Observ. **58**: 168–176.
11. Jia K, Liang S, Liu S, Li Y, Xiao Z, Yao Y, Jiang B, Zhao X, Wang X, Xu S and Cui J, 2015. Global land surface fractional vegetation cover estimation using general regression neural networks from MODIS surface reflectance. IEEE Trans. Geosci. Remote Sens. **53**: 4787–4796.
12. Jia K, Li Y, Liang S, Wei X, Mu X and Yao Y, 2017. Fractional vegetation cover estimation based on soil and vegetation lines in a corn-dominated area. Geocarto Int. **32**: 531–540.
13. Vozhehova R, Maliarchuk M, Biliaieva I, Lykhovyd P, Maliarchuk A and Tomnytskyi A, 2020. Spring row crops productivity prediction using normalized difference vegetation index. JEE. **21**: 176–182.
14. Li Z, Chen Z, Cheng Q, Duan F, Sui R, Huang X and Xu H, 2022. UAV-based hyperspectral and ensemble machine learning for predicting yield in winter wheat. Agronomy. **12**: 202.
15. McCool C, Beattie J, Milford M, Bakker J D, Moore J L and Firn J, 2018. Automating analysis of vegetation with computer vision: cover estimates and classification. Ecol. Evol. **8**: 6005–6015.
16. Bauer T and Strauss P, 2014. A rule-based image analysis approach for calculating residues and vegetation cover under field conditions. Catena. **113**: 363–369.
17. Sohail M F, Leow C Y and Won S, 2018. Non-orthogonal multiple access for unmanned aerial vehicle assisted communication. IEEE Access. **6**: 22716–22727.
18. Sun Z, Wang X, Wang Z, Yang L, Xie Y and Huang Y, 2021. UAVs as remote sensing platforms in plant ecology: review of applications and challenges. J. Plant. Ecolog. **14**: 1003–1023.
19. Kim I H, Jeon H, Baek S C, Hong W H and Jung H J, 2018. Application of crack identification techniques for an aging concrete bridge inspection using an unmanned aerial vehicle. Sensors. **18**: 1881.
20. Chiang K W, Tsai M L, Naser E S, Habib A and Chu C H, 2015. A new calibration method using low cost MEM IMUs to verify the performance of UAV-borne MMS payloads. Sensors. **15**: 6560–6585.
21. Lykhovyd P V, Vozhehova R A, Lavrenko S O and Lavrenko N M, 2022. The study on the relationship between normalized difference vegetation index and fractional green canopy cover in five selected crops. Sci. World J. **2022**: 8479424.
22. Choi S K, Lee S K, Jung S H, Choi J W, Choi D Y and Chun S J, 2016. Estimation of fractional vegetation cover in sand dunes using multi-spectral images from fixed-wing UAV. JKSGPC. **34**: 431–441.

23. Liu Y H, Cai Z L and Bao N S, 2018. Research of grassland vegetation coverage and biomass estimation method based on major quadrat from UAV photogrammetry. Ecol. Environ. **27**: 2023–2032.
24. Xie B, Yang W and Wang F, 2020. A new estimation method for fractional vegetation cover based on UAV visual light spectrum. Sci. Surv. Mapp. **45**: 72–77.
25. Hague T, Tillett N D and Wheeler H, 2006. Automated crop and weed monitoring in widely spaced cereals. Precis. Agricult. **7**: 21–32.
26. Zhang D, Mansaray L R, Jin H, Sun H, Kuang Z and Huang J, 2018. A universal estimation model of fractional vegetation cover for different crops based on time series digital photographs. Comput. Electron. Agr. **151**: 93–103.
27. Torres-Sánchez J, Peña JM, de Castro A I and López-Granados F, 2014. Multi-temporal mapping of the vegetation fraction in early-season wheat fields using images from UAV. Comput. Electron. Agr. **103**: 104–113.
28. Liu H, Qi Y, Xiao W, Tian H, Zhao D, Zhang K, Xiao J, Lu X, Lan Y, Zhang Y, 2022. Identification of male and female parents for hybrid rice seed production using UAV-based multispectral imagery. Agriculture. **12**: 1005.
29. Guijarro M, Pajares G, Riomoros I, Herrera P J, Burgos-Artizzu X P and Ribeiro A, 2011. Automatic segmentation of relevant textures in agricultural images. Comput. Electron. Agr. **75**: 75–83.
30. Guo Y, Fu Y H, Chen S, Bryant C R, Li X, Senthilnath J, Sun H, Wang S, Wu Z and de Beurs K, 2021. Integrating spectral and textural information for identifying the tasseling date of summer maize using UAV based RGB images. Int. J. Appl. Earth Observ. **102**: 102435.
31. Xiaoqin W, Miaomiao W, Shaoqiang W and Yundong W, 2015. Extraction of vegetation information from visible unmanned aerial vehicle images. TCSAE. **31**: 152–159.
32. Sellaro R, Crepy M, Trupkin S A, Karayekov E, Buchovsky A S, Rossi C and Casal J J, 2010. Cryptochrome as a sensor of the blue/green ratio of natural radiation in Arabidopsis. Plant Physiol. **154**: 401–409.
33. Qi J, Chehbouni A, Huete A R, Kerr Y H and Sorooshian S, 1994. A modified soil adjusted vegetation index. Remote Sens. Environ. **48**: 119–126.

Yun Jiang, Jun Wang and Jiwen Yang. 2023. Estimation of fractional coverage of alpine black soils by soybean vegetation using UAV-based multi-spectral images and vegetation indices.
Ukr.J.Phys.Opt. 24: 135 – 154. doi: 10.3116/16091833/24/2/135/2023

Анотація. *Щоб одержати точно та швидко фракційне рослинне покриття (ФРП) для посівів сої в альпійських чорноземних регіонах на стадіях цвітіння та наповнення насінням, ми використали безпілотні літальні апарати (БПЛА) для збору мультиспектральних зображень посівів сої. Проаналізовано та порівняно різні індекси рослинності для багатоспектральних діапазонів. Це індекс рослинності (VEG), колірний індекс вилучення рослинності (CIVE), індекс надмірної зеленості (EXG), індекс надмірної зелено-червоної різниці (EXGR), комбінований індекс рослинності (CVI), нормалізований індекс зелено-блакитної різниці (NGBDI), нормалізований індекс рослинності (NDVI), індекс рослинності з поправкою на ґрунт (SAVI) та модифікований індекс рослинності з поправкою на ґрунт (MSAVI). Контрольований метод класифікації поєднано з пороговим методом на основі статистичних гістограм індексів рослинності. Це пропонує ефективну техніку для встановлення покриття соєю альпійських чорноземів. Ми поділили наше експериментальне поле на пікселі ґрунту та пікселі сої, тоді як дані дистанційного зондування на основі БПЛА поділено на категорії ґрунту та соєвої рослинності за допомогою контрольованого методу класифікації. Потім перетини гістограм розподілу індексів рослинності, одержаних за допомогою даних БПЛА, беруть як порогові*

значення для пікселів ґрунту та рослинності. ФРП сої, одержаний із синхронно зібраних зображень високої чіткості у видимому світлі з базовою роздільною здатністю 0,036 м, використано як еталонне значення для порівняльного аналізу точностей. Наше дослідження засвідчило таке: (1) точність встановлення ФРП стає вищою за 90%, якщо поріг індексу рослинності визначають за допомогою статистичних гістограм, а зображення, отримані за допомогою БПЛА, класифікують для знаходження ФРП; (2) за допомогою індексу NGBDI одержуємо занадто високе ФРП; похибки дорівнюють 6,14% і 2,18% відповідно для етапів цвітіння-сіву та висипання насіння; (3) індекси COM, VEG, EXG, SAVI та MSAVI демонструють достатню точність і надійність; (4) індекс EXG забезпечує найвищу точність на стадії стручкування, тоді як індекс COM є найліпшим для періоду наповнення соєвими зернами. Наші результати є важливим орієнтиром для майбутніх високоточних досліджень рослинного покриву сої на різних стадіях росту.

***Ключові слова**: багатоспектральні зображення, посіви сої, індекси рослинності, безпілотні літальні апарати (БПЛА).*